Unidirectional evanescent-wave coupling from circularly polarized electric and magnetic dipoles: An angular spectrum approach

Michela F. Picardi,[1,*] Alejandro Manjavacas,[2] Anatoly V. Zayats,[1] and Francisco J. Rodríguez-Fortuño[1]

[1]*Department of Physics, King's College London, Strand, London WC2R 2LS, United Kingdom*

[2]*Department of Physics and Astronomy, University of New Mexico, Albuquerque, New Mexico 87131, United States*

(Received 13 December 2016; revised manuscript received 17 May 2017; published 16 June 2017)

Unidirectional evanescent-wave coupling from circularly polarized dipole sources is one of the most striking types of evidence of spin-orbit interactions of light and an inherent property of circularly polarized dipoles. Polarization handedness self-determines propagation direction of guided modes. In this paper, we compare two different approaches currently used to describe this phenomenon: the first requires the evaluation of the coupling amplitude between dipole and waveguide modes, while the second is based on the calculation of the angular spectrum of the dipole. We present an analytical expression of the angular spectrum of dipole radiation, unifying the description for both electric and magnetic dipoles. The symmetries unraveled by the implemented formalism show the existence of specific terms in the dipole spectrum which can be recognized as being directly responsible for directional evanescent-wave coupling. This provides a versatile tool for both a comprehensive understanding of the phenomenon and a fully controllable engineering of directionality of guided modes.

DOI: 10.1103/PhysRevB.95.245416

I. INTRODUCTION

The nanophotonics and quantum optics communities have recently shown strong interest in the fascinating scenario of a photonic waveguide being excited by a circularly polarized electric dipole source showing strong directionality [1–8]. The practical importance of the unidirectional excitation by circularly polarized dipoles is evident in quantum optics, as it provides a means of mapping quantum spin states into different free-photon states [7–13]. It is also extremely interesting in classical nanophotonics, where the dipole scattering can be imitated by a small illuminated particle in the Rayleigh limit. Small particles illuminated with circularly polarized light behave as circularly polarized dipolar scatterers and thus exhibit directional excitation of modes in nearby waveguides [14–17]. The effect is an example of spin-orbit interaction (SOI) of light, where light polarization determines the light propagation trajectory [18,19]. SOI effects are generally believed to be small unless enhanced with artificial materials [20,21]. However, in the present case, illuminated particles scatter light into completely opposite directions, constituting a remarkably simple yet drastic example of SOI, providing a unique opportunity for robust, integrated, ultrafast light nanorouting based on polarization [15,22–25]. The effect can also have important consequences in the optical manipulation of chiral [26,27] and nonchiral nanoparticles [28–31], giving rise to unintuitive lateral forces, as well as applications in optical isolation [13,32].

Different approaches are commonly used to explain the unidirectionality effect of dipolar scattering. A very general and simple one relies on the fact that the coupling strength of a dipole to any photonic mode is proportional to the similarity between the electric dipole vector $\mathbf{p}$ and the electric field vector of the photonic mode at the location of the dipole $\mathbf{E}(\mathbf{r}_0)$. Therefore, the dipole can be made to match the fields of the mode propagating in one direction but not the opposite one [3–9]. This line of thought can be equally well applied to magnetic dipoles [5,7]. Another approach relies on the asymmetric near-field angular spectrum of dipole fields themselves, together with considerations of momentum conservation [1,2,15,16]. This approach applies only to the case of planar waveguides but provides very valuable physical insight. It shows that the directionality of a circularly polarized dipole is a property of its evanescent components that can be observed only when the dipole is placed in close proximity to a structure. The case of magnetic dipole directionality, although already considered in the first approach, has never been treated analytically with spectral calculations. The knowledge of the angular spectra of magnetic dipoles is important for the design of dielectric-based nanophotonic systems since magnetic dipoles can experimentally be achieved by illuminating high-index spheres of dimensions comparable to fractions of a wavelength [33,34], whose lowest-order resonance has a magnetic dipole character. In this paper, we derive the analytical angular spectra of both electric and magnetic dipoles in a concise nomenclature, which provides an intuitive straightforward understanding of their scattering directionality. We also show in a simple way how both explanations discussed above: (i) mode coupling and (ii) the dipole angular spectrum, are ultimately equivalent in the scenarios where both apply.

II. MODE COUPLING AND SPIN-DIRECTION LOCKING

We start with a very brief overview of the mode-coupling explanation of directional scattering of circularly polarized dipoles [4–9]. Consider a dipolar emitter located in $\mathbf{r}_0$ close to a waveguide interface (outside or inside the waveguide). In the most general case, the emitter can have nonzero electric $\mathbf{p}$ and magnetic $\mathbf{m}$ dipole moments.

The probability that photons emitted by the source couple to a certain waveguide mode is proportional to the square modulus of the coupling amplitude between the dipole moments and the mode fields in the waveguide [3–5],

$$P \propto |\mathbf{p}^* \cdot \mathbf{E}(\mathbf{r}_0) + \mathbf{m}^* \cdot \mu \mathbf{H}(\mathbf{r}_0)|^2, \tag{1}$$

where $\mathbf{p}$ and $\mathbf{m}$ are electric and magnetic dipole moments, μ is the magnetic permeability of the medium, and $\mathbf{E}(\mathbf{r}_0)$

*Corresponding author: michela.picardi@kcl.ac.uk

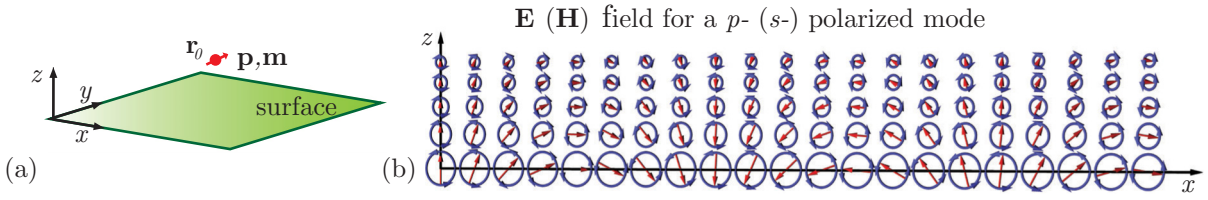

FIG. 1. (a) Schematic of an electric or magnetic dipole placed near a surface. (b) Electric (magnetic) field of a p-polarized (s-polarized) evanescent wave propagating in the $+x$ direction. It corresponds, for example, to the electric field of surface plasmon polaritons, which is p polarized, or to the magnetic field of an s-polarized guided mode on a dielectric slab. Red arrows depict the instantaneous field amplitude, while blue lines show the corresponding polarization ellipses.

and $\mathbf{H}(\mathbf{r}_0)$ are electric and magnetic fields calculated at $\mathbf{r} = \mathbf{r_0}$, respectively. This expression is valid for any type of wave-guided mode, provided that fields at $\mathbf{r}_0$ are known. It can be verified that there are positions at which the modes of a waveguide display circularly (or, more generally, elliptically) polarized fields with a handedness that depends on the propagation direction. These positions can either lie inside the waveguide [6–8] or be in its close proximity, in the regions of evanescent tails that surround it [3–5,9,35]. Hence, it follows that circularly (or elliptically) polarized dipoles with opposite handedness will couple into opposite propagating directions of the modes, while linearly polarized dipoles will excite them equally in both directions [9]. This can occur for modes of optical fibers [14,36,37], integrated optical waveguides [4,6], plasmonic waveguides [1], and photonic crystal waveguides for both electric and magnetic dipole sources [7].

We consider the simple scenario of a dipole near planar waveguides, slabs, or surfaces, with faces perpendicular to the z axis [see Fig. 1(a)]. In this simple case, the modes supported by the structure can be analytically described. Furthermore, we can assume $k_y = 0$ without loss of generality and therefore deal with a two-dimensional problem. The guided modes of such systems, in the region $z > 0$, are time-harmonic evanescent waves oscillating at a frequency ω and characterized by a wave vector $\mathbf{k}^{\pm} = (k_x, k_y = 0, \pm k_z)$, where $k_z = \sqrt{k^2 - k_x^2}$, $k = n\omega/c$, and $n = c\sqrt{\varepsilon\mu}$ is the refractive index of the surrounding medium. The positive sign in k_z assumes evanescent decay in the $+\hat{\mathbf{z}}$ direction (the opposite case can be obtained by reversing the sign of k_z). If we assume a real n, evanescent waves fulfill $\mathrm{Re}(k_x) > k$, resulting in k_z having an imaginary component. The evanescent wave field is written as

$$\mathbf{E}(\mathbf{r}) = \mathbf{E}_0 e^{i\mathbf{k}^{\pm}\cdot\mathbf{r}}.$$

Using the expressions $\mathbf{H} = \frac{1}{\omega\mu}(\mathbf{k}^{\pm} \times \mathbf{E})$, $\mathbf{E} = -\frac{1}{\omega\varepsilon}(\mathbf{k}^{\pm} \times \mathbf{H})$, directly derived from Maxwell's equations, and the subsequent transversality conditions $\mathbf{E}\cdot\mathbf{k}^{\pm} = 0$ and $\mathbf{H}\cdot\mathbf{k}^{\pm} = 0$, we obtain the electric and magnetic fields of p-polarized (TM) and s-polarized (TE) evanescent modes [2,5,38,39]:

$$\begin{aligned} \mathbf{E}_0^p &= \begin{pmatrix} \pm k_z A_{\mathrm{TM}} \\ 0 \\ -k_x A_{\mathrm{TM}} \end{pmatrix}, \quad \mathbf{H}_0^p = \frac{k^2}{\omega\mu}\begin{pmatrix} 0 \\ A_{\mathrm{TM}} \\ 0 \end{pmatrix}, \\ \mathbf{E}_0^s &= -\frac{k^2}{\omega\varepsilon}\begin{pmatrix} 0 \\ A_{\mathrm{TE}} \\ 0 \end{pmatrix}, \quad \mathbf{H}_0^s = \begin{pmatrix} \pm k_z A_{\mathrm{TE}} \\ 0 \\ -k_x A_{\mathrm{TE}} \end{pmatrix}, \end{aligned} \tag{2}$$

with A_{TM} and A_{TE} being the amplitudes of the fields.

It is evident that for $\mathrm{Re}(k_x) \gg k$ the vectors associated with the complex numbers k_x and k_z become almost orthogonal to one another in the complex plane, so that $\mathbf{E}^p$ and $\mathbf{H}^s$ fields are elliptically polarized [see Fig. 1(b)]. In the limit in which $k_x \to \infty$, $k_z \to ik_x$, and the polarization becomes purely circular. Therefore, the basic electromagnetic equations above require that the polarization of evanescent waves is elliptical or circular in the plane of propagation. While this is not new [40], only recently was it pointed out that it implies a transverse spin angular momentum with a handedness that depends only on the propagation direction (called spin-direction or spin-momentum locking) [37,38,41,42]. This provides a very intuitive explanation for the directional excitation of evanescent waves [3,5,9,38]. If we consider an electric dipole circularly polarized in the xz plane, with the sign of the z component determining the handedness,

$$\mathbf{p}_{L,R} = \begin{pmatrix} 1 \\ 0 \\ \pm i \end{pmatrix},$$

for a p-polarized evanescent wave, when $k_x \to \infty$ with the evanescent decay in the $+z$ direction (taking the positive root for $k_z \approx ik_x$), the value of $|\mathbf{p}^* \cdot \mathbf{E}^p|$ is equal to

$$|\mathbf{p}^* \cdot \mathbf{E}^p| = \begin{cases} 0 & \text{for the propagation direction } \mp x, \\ 2E_x & \text{for the propagation direction } \pm x, \end{cases}$$

with the sign depending only on the sign of p_z and therefore explaining the directionality. It is interesting to verify that the value of the product $|\mathbf{p}^* \cdot \mathbf{E}^p|$ does not result in directional emission if the wave is propagating ($|k_x| \leqslant k$) instead of evanescent ($|k_x| > k$) or, likewise, if the dipole is linearly polarized.

Similar considerations apply to the case of a circularly polarized magnetic dipole coupled with the magnetic field $\mathbf{H}^s$ of an s-polarized evanescent wave.

III. DIPOLE ANGULAR SPECTRUM APPROACH

The focus of this work is on an alternative explanation for the directionality of the emission of circularly polarized dipoles based on the angular spectrum (momentum representation) of the emitted waves. This explanation was introduced in [1] for only electric dipoles. Here we provide a simplified analytical formulation of this approach that presents advantages in terms

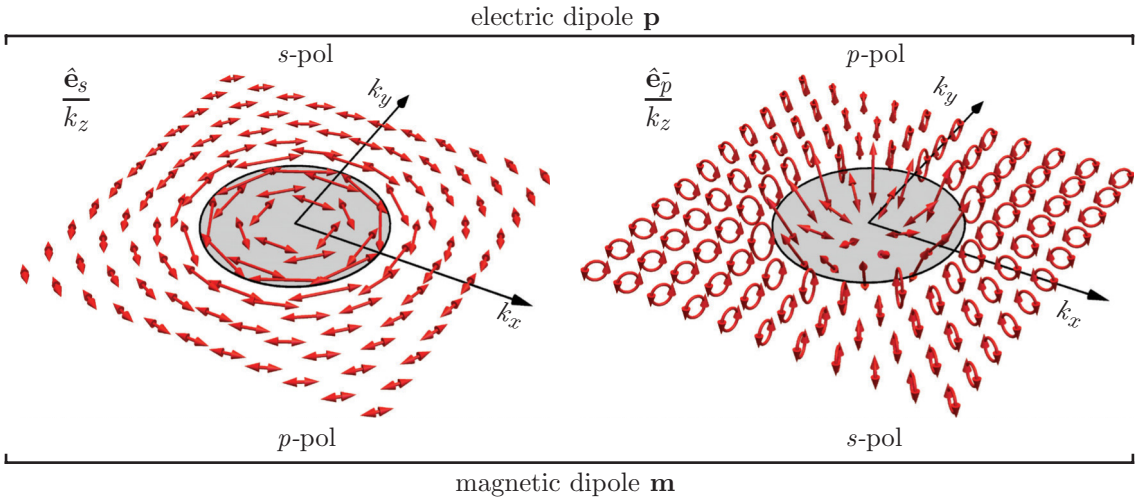

FIG. 2. Electric field polarization associated with $(\hat{\mathbf{e}}_s/k_z)$ and $(\hat{\mathbf{e}}_p^-/k_z)$ as a function of k_x and k_y. The shaded areas correspond to the propagating components $k_x^2 + k_y^2 < k^2$. The polarization ellipse associated with a complex vector $\mathbf{v}$ is computed as the parametric curve defined by $\mathrm{Re}(\mathbf{v}e^{-i\omega t})$. While $\hat{\mathbf{e}}_s$ is associated with linear polarization for any value of k_x and k_y and does not give rise to any directionality, $\hat{\mathbf{e}}_p^{\pm}$ is associated with elliptical polarization for the evanescent components ($|k_t| > k$) and linear polarization for propagating components ($|k_t| < k$).

of both physical intuition and system design engineering. Also, we extend it to the case of magnetic dipoles.

We start by considering an arbitrary electric dipole $\mathbf{p}$ located at $\mathbf{r}_0 = (0,0,z_0)$ within a homogeneous medium with permittivity ε, permeability μ, and wave number $k = \omega\sqrt{\varepsilon\mu}$. The electric field $\mathbf{E}^{\mathrm{ED}}$ generated by the dipole can be expressed using the angular spectrum as [43]

$$\mathbf{E}^{\mathrm{ED}}(x,y,z) = \iint \mathbf{E}^{\mathrm{ED}}(k_x,k_y)|_{z=z_0} \times e^{i(k_x x + k_y y + k_z|z-z_0|)} dk_x dk_y.$$

We can project $\mathbf{E}^{\mathrm{ED}}(k_x,k_y)|_{z=z_0}$ on $\hat{\mathbf{e}}_s$ and $\hat{\mathbf{e}}_p^{\pm}$ [44], which are the unit vectors of the electric field of s-polarized and p-polarized waves, defined as (see Appendix A)

$$\hat{\mathbf{e}}_s(k_x,k_y) = \left(-\frac{k_y}{k_t}, \frac{k_x}{k_t}, 0\right),$$
$$\hat{\mathbf{e}}_p^{\pm}(k_x,k_y) = \left(\pm\frac{k_x k_z}{k k_t}, \pm\frac{k_y k_z}{k k_t}, -\frac{k_t}{k}\right),$$

where $k_t = \sqrt{k_x^2 + k_y^2}$ and the $+$ and $-$ symbols account for fields calculated above and below $z = z_0$, respectively.

Applying this decomposition (see Appendix B for details), it is possible to write the angular spectrum of the field as the sum of s- and p-polarized components:

$$\mathbf{E}^{\mathrm{ED}}(k_x,k_y)|_{z=z_0} = \frac{ik^2}{8\pi^2\varepsilon}\frac{1}{k_z}[(\hat{\mathbf{e}}_s \cdot \mathbf{p})\hat{\mathbf{e}}_s + (\hat{\mathbf{e}}_p^{\pm} \cdot \mathbf{p})\hat{\mathbf{e}}_p^{\pm}]. \quad (3)$$

In the same way, for a magnetic dipole with arbitrary dipole moment $\mathbf{m}$ (see Appendix C), we can write its electric field angular spectrum as

$$\mathbf{E}^{\mathrm{MD}}(k_x,k_y)|_{z=z_0} = -\frac{ik^2}{8\pi^2\varepsilon}\frac{1}{k_z}\frac{1}{c}[(\hat{\mathbf{e}}_p^{\pm} \cdot \mathbf{m})\hat{\mathbf{e}}_s - (\hat{\mathbf{e}}_s \cdot \mathbf{m})\hat{\mathbf{e}}_p^{\pm}]. \quad (4)$$

These compact equations are the main result of this work, written in vector form, independent of basis representation. In previous works [43–45], the angular spectra of dipoles were calculated in terms of matrix elements of the Green's tensor in a given coordinate system. These matrix elements are difficult to associate with an intuitive interpretation. Equations (3) and (4) instead provide physical insight, unravel symmetries in the fields, and prove to be useful design rules. They allow for a direct understanding of the effect of spin-momentum locking in relation to dipole evanescent-wave excitation. Examining them, we see that the p-polarized angular spectrum of an electric dipole $\mathbf{p}$ is given directly (up to a constant prefactor) by $(\hat{\mathbf{e}}_p^{\pm}/k_z) \cdot \mathbf{p}$, identical in form to the s-polarized field of a magnetic dipole $(\hat{\mathbf{e}}_p^{\pm}/k_z) \cdot \mathbf{m}$. Analogously, the s-polarized field of an electric dipole is given by $(\hat{\mathbf{e}}_s/k_z) \cdot \mathbf{p}$, while the p-polarized field of a magnetic dipole reads $(\hat{\mathbf{e}}_s/k_z) \cdot \mathbf{m}$. Therefore, the simple operations $[(\hat{\mathbf{e}}_p^{\pm}/k_z)\cdot]$ and $[(\hat{\mathbf{e}}_s/k_z)\cdot]$ acting on electric and magnetic dipole moments provide all the information about their near-field and far-field directionality.

In Fig. 2, we plot the polarization ellipse associated with the complex vectors $(\hat{\mathbf{e}}_s/k_z)$ and $(\hat{\mathbf{e}}_p^-/k_z)$ as functions of k_x and k_y. The figure provides a simple guideline for the design of dipole directionality at a glance. It also unifies the spectra of electric and magnetic dipoles, highlighting that they have identical directionality but applied to different mode polarizations. Applying the dot product between these vectors and the dipole moments $\mathbf{p}$ or $\mathbf{m}$, following Eqs. (3) and (4), we obtain the p-polarized and s-polarized components of the electric and magnetic dipoles. The dot product between two complex vectors $\mathbf{u} \cdot \mathbf{v}$ is maximum when $\mathbf{u} \propto \mathbf{v}^*$, as derived by Schwarz's inequality. Therefore, it is possible to engineer the dipole moment $\mathbf{p}$ or $\mathbf{m}$ to maximize (minimize) its angular spectrum components at a specific transverse wave vector (k_x,k_y), simply by maximizing (minimizing) its scalar product with the vector $(\hat{\mathbf{e}}_p^{\pm}/k_z)$.

The spectra of a circularly polarized dipole are shown in Fig. 3, calculated by applying the $[(\hat{\mathbf{e}}_p^-/k_z)\cdot]$ and $[(\hat{\mathbf{e}}_s/k_z)\cdot]$

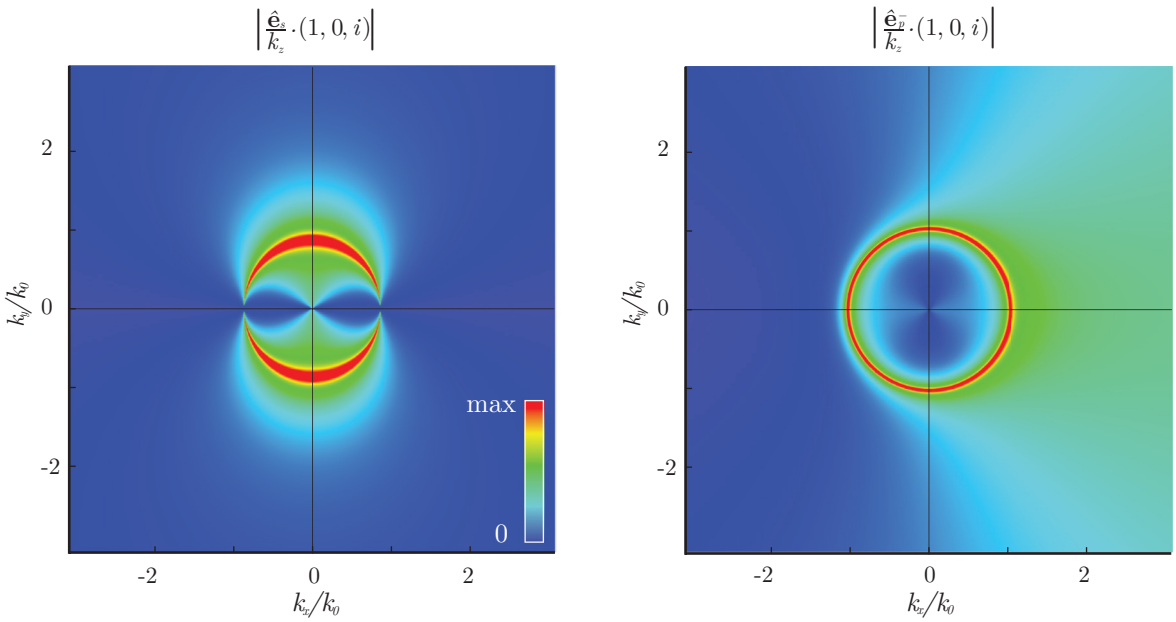

FIG. 3. Angular spectrum of s- and p-polarized components of the electric field on the plane (k_x,k_y) generated by a circularly polarized dipole $\mathbf{p} = [1,0,i]$.

operations to the dipole vectors $\mathbf{p}$ or $\mathbf{m} = (1,0,i)$. When $k_t \to \infty$, $(\hat{\mathbf{e}}_p^{\pm}/k_z)$ approaches circular polarization, which in turn means that the circularly polarized dipole will maximize the scalar product along one direction while simultaneously minimizing it along the exactly opposite one. This happens only for the p-polarized fields of an electric dipole or the s-polarized fields of a magnetic one (i.e., the terms that involve $\hat{\mathbf{e}}_p^{\pm}$). No directionality can be observed in the other terms, (i.e., those that involve $\hat{\mathbf{e}}_s$), which is true in general because the vector $(\hat{\mathbf{e}}_p^{\pm}/k_z)$ changes under the inversion $(k_x,k_y) \to (-k_x,-k_y)$, while the vector $(\hat{\mathbf{e}}_s/k_z)$ does not, except for a global phase factor. Therefore, this inversion does not affect the polarization associated with $\hat{\mathbf{e}}_s$, indeed modifying the one associated with $\hat{\mathbf{e}}_p^{\pm}$

We would like to emphasize that all the discussion above relates only to the angular components of the dipole itself in a homogeneous medium, with no mention being made of nearby surfaces or waveguides. However, when a dipole is placed in close proximity to a surface, it is clear that, due to the conservation of transverse momentum, the probability of excitation of the waveguide modes will necessarily be proportional to the amplitude of the angular spectrum of the dipole at the specific (k_x,k_y) of each waveguide mode [1], weighted by the corresponding Fresnel reflection coefficients containing information about the s-polarized and p-polarized modes existing at the surface. The precise mathematical formulation of this is given in Appendix D. This means that when a dipole displaying a strongly asymmetric spectrum in its evanescent components (such as that in Fig. 3) is placed in near-field proximity to a surface or planar waveguide, unidirectional excitation of guided modes will take place. This conclusion is reached independently of the field structure of the guided modes. A similar argument can be made in a nonplanar waveguide in which only one direction of space is translationally invariant, such as an optical fiber. In that case, only one wave-vector component (along the waveguide direction, e.g., k_x) is conserved, but we can use logic similar to that above to conclude that directional excitation will take place due to the asymmetry of the spectrum in k_x. An example of this can be seen in Fig. 4, where a waveguide with a nonanalytical cross section is directionally excited by a circular dipole.

One of the advantages of knowing the angular spectrum is the possibility to calculate the fields at every point of space by integrating the expressions above, with the reflected counterparts given in Appendix D. As an example, in Fig. 5

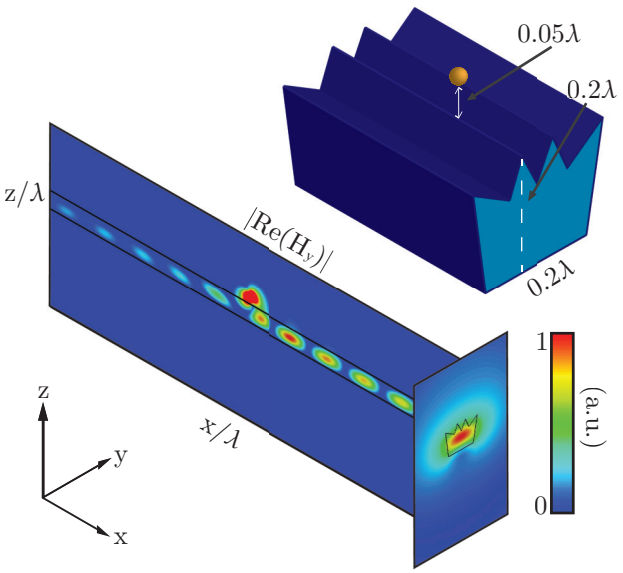

FIG. 4. Directional excitation of guided modes in a nonplanar waveguide with a nonanalytically solvable cross section. The refractive index of the waveguide material is $n = 3$ and the surrounding medium is air. A circular dipole $\mathbf{p} = [1,0,i]$ is placed between the central ribs of the waveguide, and the smallest distance between the dipole and the waveguide profile is 0.05λ.

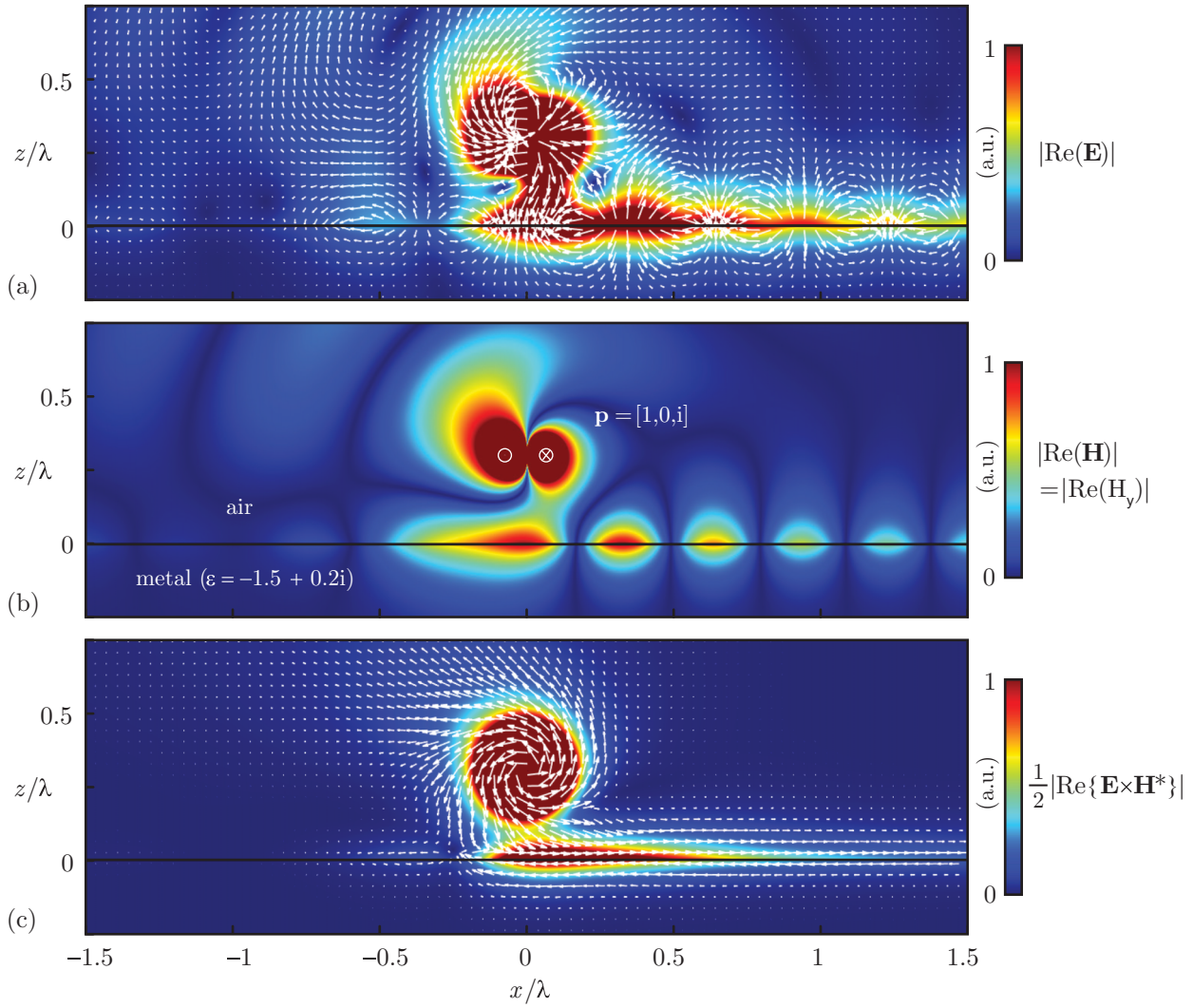

FIG. 5. (a) and (b) Electromagnetic field and (c) power flow induced by a circularly polarized electric (magnetic) dipole in close proximity to an interface of a material with $\varepsilon = -1.5 + 0.2i$ and $\mu = 1$ ($\mu = -1.5 + 0.2i$ and $\varepsilon = 1$), calculated by integration of the angular spectra of the dipole field given by Eq. (3) added to the reflected fields given by Eq. (D1). The color map represents amplitude, and white arrows represent the direction of (a) instantaneous electric (magnetic) field, (b) instantaneous magnetic (electric) field, and (c) the time-averaged Poynting vector. Snapshots from Supplemental Movie M1 [46].

we show the electric field, magnetic field, and time-averaged Poynting vector for a circular electric dipole placed in close proximity to a metallic surface supporting surface plasmon polariton modes. An animated version is provided in the Supplemental Material as Movie M1 [46].

Far-field and near-field directionality

The asymmetry in the evanescent angular spectrum components of circular dipoles ($|k_x| > k$) is in strong contrast to the symmetry of the propagating angular spectrum components ($|k_x| \leqslant k$). In fact, circular dipole antennas are commonly used in radio frequency to avoid directional emission because they do not present any preferred radiation direction in the plane of the dipole. The sharp contrast in the behavior between the evanescent and propagating components can be explained by simple superposition arguments.

In Fig. 6 we plot the p-polarized (s-polarized) angular spectra of electric (magnetic) dipoles along k_x, assuming $k_y = 0$. This corresponds to the term responsible for unidirectionality, given by $[\hat{\mathbf{e}}_p^-(k_x, k_y = 0)/k_z] \cdot \mathbf{p} = (1/k)(-1,0, -k_x/k_z) \cdot (p_x, p_y, p_z)$. We can easily see that the angular spectrum of a vertical dipole is an odd function of k_x [Fig. 6(a)], while that of a horizontal dipole is even [Fig. 6(b)]. The superposition of both components can therefore be a strongly asymmetric function of k_x. However, the superposition gives completely different results depending on the phase difference between the two of them. For instance, in a diagonal linearly polarized dipole $\mathbf{p} = (1,0,1)$ the evanescent angular frequency spectrum components ($|k_x| > k$) have the same amplitude in both directions ($\pm k_x$). On the other hand, a circularly polarized dipole as discussed above introduces a $\pi/2$ phase between the two components, $\mathbf{p} = (1,0,i)$, and the resulting evanescent angular frequency spectrum ($|k_x| > k$) is highly nonsymmetric, accounting for circular

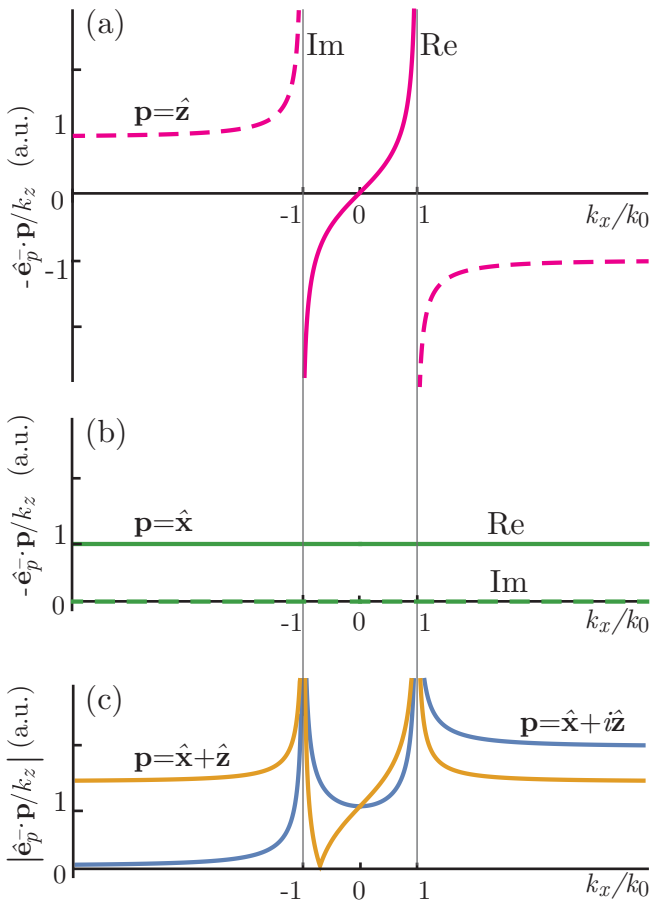

FIG. 6. Angular spectra along k_x ($k_y = 0$) of (a) vertically polarized, (b) horizontally polarized, and (c) diagonally polarized (yellow) and circularly polarized (blue) dipoles. In (c) the absolute values of the angular spectra are plotted. Note that the spectra plotted represent the amplitude density per unit k_x/k_0. To obtain the radiation diagram it should be converted to amplitude density per unit angle, using the relation $dk_x = k_0 \cos\theta d\theta$.

dipole directionality [Fig. 6(c)]. It should be noticed that the exact opposite behavior takes place for the propagating components ($|k_x| \leqslant k$), where the spectrum of the circular dipole has a symmetric amplitude in k_x, while that of a linear dipole is strongly asymmetric (corresponding to the radiation diagrams of circular and linear dipoles).

The different behavior in the spectra of evanescent and propagating components of a dipole intuitively allows for a complete understanding of the reason why directionality of circularly polarized dipoles is observed only when the waveguide is placed in a region of near fields, where the evanescent components are non-negligible. In fact, the directionality is a property belonging only to the evanescent part of the dipole angular spectrum and can therefore be observed when the evanescent components are coupled to a waveguide mode. Further evidence of the directionality of the dipole near fields can be seen in the time-averaged Poynting vector of a circularly polarized electric dipole [Fig. 5(c)]. We can see that the energy flow is circulating around the dipole in its near-field region in the same sense as the dipole rotation, intuitively explaining why surface waves will be excited directionally in the nearby plasmonic surface. In contrast, the Poynting vector becomes radial in the far field of the dipole.

IV. CONCLUSIONS

We compared two different descriptions of the phenomenon of directional excitation of guided modes driven by electric and magnetic dipoles. The two explanations look profoundly different in nature because the first one depends explicitly on the waveguide-mode field structure, while the second one depends only on the dipole fields and on momentum conservation. The second description has the advantage of showing explicitly that the circularly polarized dipole directionality is a universal phenomenon, in the sense that the same dipole can unidirectionally excite any waveguide mode with the appropriate wave vector, as directionality is determined by the dipole itself. Both considered approaches lead to identical results. The reason behind this equivalence lies in the fact that, as shown in Eq. (2), for guided modes the field structure can be completely described once its wave vector has been specified and, conversely, given the field structure, the associated wave vector is completely determined. While the mode-coupling explanation focuses on how the field-vector structure of the modes matches the field of the dipole, the angular spectrum explanation focuses on how the wave vector of the modes matches those of the dipole. Ultimately, the two explanations of the phenomenon are formally equivalent. Other explanations of the effect have been proposed considering the quantum spin Hall effect as an intrinsic property of Maxwell's equations [38]. Controlling directionality exclusively with light polarization allows ultrahigh-speed modulation and switching of light, with broadband behavior, opening new avenues for light nanorouting based on a very fundamental concept that works in a variety of platforms ranging from microwaves to nanophotonics and plasmonics. Dipole directionality also provides a method for readout of quantum spin states mapped into photons propagating on different directions. The knowledge of the angular spectrum of dipoles in the form presented here greatly helps in understanding their directionality properties and provides a simple recipe for engineering the required electric or magnetic dipole moments to achieve directional excitation of any mode in planar waveguides by simply knowing the dispersion of the mode and its polarization (s or p). By including the magnetic dipole in our analysis, we enable the analytical design of applications requiring directional excitation of s-polarized modes. The simultaneous excitation of electric and magnetic dipoles in a single particle is known to enable remarkable directionality properties such as reduced backscattering and can be experimentally achieved in particles with overlapping electric and magnetic resonances using high-index dielectric particles [47–50]. Our compact notation allows the straightforward calculation of the angular spectrum in both propagating and evanescent components of simultaneous electric and magnetic dipoles with arbitrary polarizations.

ACKNOWLEDGMENTS

This work was supported by European Research Council project ERC-2016-STG-714151-PSINFONI and EPSRC

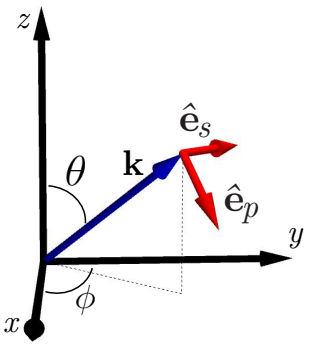

FIG. 7. Coordinate system and polarization basis used.

(UK). A.M. acknowledges financial support from the Department of Physics and Astronomy and the College of Arts and Sciences of the University of New Mexico. A.Z. acknowledges support from the Royal Society and the Wolfson Foundation. All data supporting this research are provided in full in the results section and appendices.

APPENDIX A: POLARIZATION VECTOR BASIS

For our calculations we always use vectors $\hat{\mathbf{e}}_s(k_x,k_y)$ and $\hat{\mathbf{e}}_p^{\pm}(k_x,k_y)$ as our basis [39]. These vectors are related to the electric field polarization in s-polarized and p-polarized fields, respectively, and can be defined as

$$\begin{aligned}\hat{\mathbf{e}}_s &= \frac{\hat{\mathbf{z}}\times\mathbf{k}^{\pm}}{\sqrt{(\hat{\mathbf{z}}\times\mathbf{k}^{\pm})\cdot(\hat{\mathbf{z}}\times\mathbf{k}^{\pm})}}\\ &= (-\sin\phi,\cos\phi,0)\\ &= \frac{1}{\sqrt{k_x^2+k_y^2}}(-k_y\hat{\mathbf{x}}+k_x\hat{\mathbf{y}}),\end{aligned} \tag{A1}$$

$$\begin{aligned}\hat{\mathbf{e}}_p^{\pm} &= \hat{\mathbf{e}}_s\times\frac{\mathbf{k}^{\pm}}{k}\\ &= (\pm\cos\theta\cos\phi,\pm\cos\theta\sin\phi,-\sin\theta)\\ &= \frac{1}{k\sqrt{k_x^2+k_y^2}}\left[\pm k_xk_z\hat{\mathbf{x}}\pm k_yk_z\hat{\mathbf{y}}-\left(k_x^2+k_y^2\right)\hat{\mathbf{z}}\right],\end{aligned} \tag{A2}$$

where k is the wave number of the medium; $\mathbf{k}^{\pm}=(k_x,k_y,\pm k_z)$ is the wave vector, with the $+$ and $-$ signs accounting for fields calculated above and below $z=z_0$, respectively; and $\hat{\mathbf{z}}$ is the unit vector normal to the plane in which we choose to expand the angular spectrum. Importantly, these vectors are valid for both near-field evanescent waves $|k_t|>k$ and far-field propagating waves $|k_t|\leqslant k$. In the propagating lossless case, $\mathbf{k}^{\pm}$ is purely real, and its magnitude is $|\mathbf{k}^{\pm}|^2=k^2$, so following the definition in Eqs. (A1) and (A2), vectors $\hat{\mathbf{e}}_s$ and $\hat{\mathbf{e}}_p^{\pm}$ are purely real unit vectors forming an orthonormal basis, as pictured in Fig. 7.

In the evanescent case, $\mathbf{k}^{\pm}$ becomes complex, and $|\mathbf{k}^{\pm}|^2=\mathbf{k}^{\pm}\cdot\mathbf{k}^{\pm *}>k^2$, which translates into the vector $\hat{\mathbf{e}}_p^{\pm}$ becoming complex and no longer having unit magnitude. However, equation $\mathbf{k}^{\pm}\cdot\mathbf{k}^{\pm}=k_x^2+k_y^2+k_z^2=k^2$ always holds [5,39], so $\hat{\mathbf{e}}_s$ and $\hat{\mathbf{e}}_p^{\pm}$ are still an "orthonormal basis" in the special sense that $\hat{\mathbf{e}}_s\cdot\hat{\mathbf{e}}_s=\hat{\mathbf{e}}_p^{\pm}\cdot\hat{\mathbf{e}}_p^{\pm}=1$ and $\hat{\mathbf{e}}_s\cdot\hat{\mathbf{e}}_p^{\pm}=0$, with no complex conjugation. This means that we can always use $\hat{\mathbf{e}}_s$ and $\hat{\mathbf{e}}_p^{\pm}$ as a valid geometrical orthonormal basis, as long as we remember that, if $\mathbf{f}=a\hat{\mathbf{e}}_s+b\hat{\mathbf{e}}_p^{\pm}$, then $a=\mathbf{f}\cdot\hat{\mathbf{e}}_s$ and $b=\mathbf{f}\cdot\hat{\mathbf{e}}_p^{\pm}$, with no complex conjugation. Also notice the simple relations $\hat{\mathbf{e}}_p^{\pm}\times\hat{\mathbf{e}}_s=(\mathbf{k}^{\pm}/k)$, $(\mathbf{k}^{\pm}/k)\times\hat{\mathbf{e}}_p^{\pm}=\hat{\mathbf{e}}_s$, and $(\mathbf{k}^{\pm}/k)\times\hat{\mathbf{e}}_s=-\hat{\mathbf{e}}_p^{\pm}$. From these relations and the requirement $\mathbf{H}=\frac{1}{\eta}[\frac{\mathbf{k}^{\pm}}{k}\times\mathbf{E}]$ derived from Maxwell's equations for plane waves it follows that any electric field $\mathbf{E}=[A\hat{\mathbf{e}}_s+B\hat{\mathbf{e}}_p^{\pm}]e^{i\mathbf{k}^{\pm}\cdot\mathbf{r}}$ is associated with a magnetic field $\mathbf{H}=[\frac{B}{\eta}\hat{\mathbf{e}}_s-\frac{A}{\eta}\hat{\mathbf{e}}_p^{\pm}]e^{i\mathbf{k}^{\pm}\cdot\mathbf{r}}$, with $\eta=(\mu/\varepsilon)^{1/2}$. This mathematical relation always holds and can be generalized to evanescent waves.

APPENDIX B: THE ANGULAR SPECTRUM OF AN ELECTRIC DIPOLE

An electric dipole, in the time harmonic case, can be described in terms of a dipole moment $\mathbf{p}$, associated with an electric current density $\mathbf{J}=-i\omega\delta^3(\mathbf{r}-\mathbf{r_0})\mathbf{p}$, where we assume an $e^{-i\omega t}$ time dependence. The electric and magnetic fields generated by this dipole in a homogeneous medium can be written as [51]

$$\mathbf{E}^{\mathrm{ED}}=k^2\boldsymbol{\pi}+\nabla(\nabla\cdot\boldsymbol{\pi}), \tag{B1}$$

$$\mathbf{H}^{\mathrm{ED}}=-i\omega\varepsilon\nabla\times\boldsymbol{\pi}, \tag{B2}$$

with k being the wave number of the medium and $\boldsymbol{\pi}$ being a vector potential, often referred to as the Hertz potential [51], which can be calculated as the product of $\mathbf{p}$ and the scalar Green's function for the Helmholtz operator [43]:

$$\boldsymbol{\pi}=\frac{\mathbf{p}}{4\pi\varepsilon}\frac{e^{ik|\mathbf{r}-\mathbf{r_0}|}}{|\mathbf{r}-\mathbf{r_0}|}.$$

Using the well-known Weyl's identity [52],

$$\frac{e^{i\mathbf{k}\cdot\mathbf{r}}}{|\mathbf{r}|}=\frac{i}{2\pi}\iint\frac{1}{k_z}e^{i(k_xx+k_yy)}e^{ik_z|z|}dk_xdk_y,$$

assuming that the electric dipole (ED) is located on the z axis, $\mathbf{r}_0=z_0\hat{\mathbf{z}}$, we can write $\boldsymbol{\pi}$ as

$$\boldsymbol{\pi}=\frac{i}{8\pi^2\varepsilon}\iint\frac{\mathbf{p}}{k_z}e^{i(k_xx+k_yy)}e^{ik_z|z-z_0|}dk_xdk_y. \tag{B3}$$

By applying Eqs. (B1) and (B2) to (B3) (note that this is equivalent to the substitution $\nabla\rightarrow i\mathbf{k}^{\pm}$), the electric field $\mathbf{E}^{\mathrm{ED}}$ and the magnetic field $\mathbf{H}^{\mathrm{ED}}$ can be written as [44]

$$\mathbf{E}^{\mathrm{ED}}=\frac{i}{8\pi^2\varepsilon}\iint\frac{1}{k_z}e^{i(k_xx+k_yy)}e^{ik_z|z-z_0|}\mathbf{g}_Edk_xdk_y,$$

$$\mathbf{H}^{\mathrm{ED}}=\frac{i\omega}{8\pi^2}\iint\frac{1}{k_z}e^{i(k_xx+k_yy)}e^{ik_z|z-z_0|}\mathbf{g}_Hdk_xdk,$$

where $\mathbf{g}_E$ and $\mathbf{g}_H$ are given by

$$\mathbf{g}_E=k^2\mathbf{p}-\mathbf{k}^{\pm}(\mathbf{k}^{\pm}\cdot\mathbf{p}),$$

$$\mathbf{g}_H=\mathbf{k}^{\pm}\times\mathbf{p},$$

with $\mathbf{k}^{\pm}$ being

$$\mathbf{k}^{+}=(k_x,k_y,k_z)\quad\text{when}\quad z>z_0,$$

$$\mathbf{k}^{-}=(k_x,k_y,-k_z)\quad\text{when}\quad z<z_0.$$

Following Ref. [44], we can then project the function $\mathbf{g}_E(k_x,k_y)$ along the two directions $\hat{\mathbf{e}}_s$ and $\hat{\mathbf{e}}_p^{\pm}$ relative to the s and p polarizations (see Appendix A):

$$\mathbf{g}_E = \gamma_s \hat{\mathbf{e}}_s + \gamma_p^{\pm}\hat{\mathbf{e}}_p^{\pm}.$$

Therefore,

$$\begin{aligned}
\gamma_s &= \mathbf{g}_E \cdot \hat{\mathbf{e}}_s \\
&= [k^2\mathbf{p} - (\mathbf{p}\cdot\mathbf{k}^{\pm})\mathbf{k}^{\pm}] \cdot \frac{1}{\sqrt{k_x^2+k_y^2}}(-k_y\hat{\mathbf{x}} + k_x\hat{\mathbf{y}}) \\
&= \frac{k^2}{\sqrt{k_x^2+k_y^2}}(-k_y p_x + k_x p_y) = k^2\hat{\mathbf{e}}_s\cdot\mathbf{p}, \\
\gamma_p^{\pm} &= \mathbf{g}_E\cdot\hat{\mathbf{e}}_p^{\pm} = [k^2\mathbf{p} - (\mathbf{p}\cdot\mathbf{k}^{\pm})\mathbf{k}^{\pm}] \\
&\quad \cdot\frac{1}{k\sqrt{k_x^2+k_y^2}}\left(\pm k_x k_z\hat{\mathbf{x}} \pm k_y k_z\hat{\mathbf{y}} - \left(k_x^2+k_y^2\right)\hat{\mathbf{z}}\right) \\
&= \pm\frac{k_z k}{\sqrt{k_x^2+k_y^2}}(k_x p_x + k_y p_y) - k\sqrt{k_x^2+k_y^2}\,p_z \\
&= k^2\hat{\mathbf{e}}_p^{\pm}\cdot\mathbf{p}.
\end{aligned}$$

Analogously, we decompose $\mathbf{g}_H$ along the directions $\hat{\mathbf{e}}_s$ and $\hat{\mathbf{e}}_p^{\pm}$, and it can be easily checked that $\mathbf{g}_H\cdot\hat{\mathbf{e}}_s = \frac{\gamma_p^{\pm}}{k}$ and $\mathbf{g}_H\cdot\hat{\mathbf{e}}_p^{\pm} = -\frac{\gamma_s}{k}$, so that we can write

$$\mathbf{g}_H = \frac{\gamma_p^{\pm}}{k}\hat{\mathbf{e}}_s - \frac{\gamma_s}{k}\hat{\mathbf{e}}_p^{\pm}.$$

With all of the above we have all the ingredients required to compose the angular spectrum of the dipole field, defined as [43]

$$\mathbf{E}^{\mathrm{ED}}(x,y,z) = \iint \mathbf{E}^{\mathrm{ED}}(k_x,k_y)|_{z=z_0} \times e^{i(k_x x + k_y y + k_z|z-z_0|)}dk_x dk_y,$$

which can be further decomposed into p and s polarizations,

$$\mathbf{E}^{\mathrm{ED}}(k_x,k_y)|_{z=z_0} = \mathbf{E}_p^{\mathrm{ED}}(k_x,k_y)|_{z=z_0} + \mathbf{E}_s^{\mathrm{ED}}(k_x,k_y)|_{z=z_0},$$

with identical notation for the magnetic field. Putting all of this together, the p-polarized fields of the electric dipole are given by

$$\mathbf{E}_p^{\mathrm{ED}}(k_x,k_y)|_{z=z_0} = \frac{i}{8\pi^2\varepsilon}k\left[\pm\frac{1}{\sqrt{k_x^2+k_y^2}}(k_x p_x + k_y p_y) - \frac{1}{k_z}\sqrt{k_x^2+k_y^2}\,p_z\right]\hat{\mathbf{e}}_p^{\pm},$$

$$\mathbf{H}_p^{\mathrm{ED}}(k_x,k_y)|_{z=z_0} = \frac{i\omega}{8\pi^2}\left[\pm\frac{1}{\sqrt{k_x^2+k_y^2}}(k_x p_x + k_y p_y) - \frac{1}{k_z}\sqrt{k_x^2+k_y^2}\,p_z\right]\hat{\mathbf{e}}_s,$$

while the s-polarized fields are

$$\mathbf{E}_s^{\mathrm{ED}}(k_x,k_y)|_{z=z_0} = \frac{i}{8\pi^2\varepsilon}k\left[\frac{k}{k_z\sqrt{k_x^2+k_y^2}}(-k_y p_x + k_x p_y)\right]\hat{\mathbf{e}}_s,$$

$$\mathbf{H}_s^{\mathrm{ED}}(k_x,k_y)|_{z=z_0} = -\frac{i\omega}{8\pi^2}\left[\frac{k}{k_z\sqrt{k_x^2+k_y^2}}(-k_y p_x + k_x p_y)\right]\hat{\mathbf{e}}_p^{\pm}.$$

This can be written in compact notation as

$$\mathbf{E}^{\mathrm{ED}}(k_x,k_y)|_{z=z_0} = \frac{i}{8\pi^2\varepsilon}\frac{k^2}{k_z}[(\hat{\mathbf{e}}_s\cdot\mathbf{p})\hat{\mathbf{e}}_s + (\hat{\mathbf{e}}_p^{\pm}\cdot\mathbf{p})\hat{\mathbf{e}}_p^{\pm}],$$

$$\mathbf{H}^{\mathrm{ED}}(k_x,k_y)|_{z=z_0} = \frac{i\omega}{8\pi^2}\frac{k}{k_z}[(\hat{\mathbf{e}}_p^{\pm}\cdot\mathbf{p})\hat{\mathbf{e}}_s - (\hat{\mathbf{e}}_s\cdot\mathbf{p})\hat{\mathbf{e}}_p^{\pm}].$$

APPENDIX C: THE ANGULAR SPECTRUM OF A MAGNETIC DIPOLE

A magnetic dipole can be described, in the time-harmonic case ($e^{-i\omega t}$ time dependence), in terms of a magnetic dipole moment $\mathbf{m}$, associated with a magnetic current density $\mathbf{J_m} = -i\omega\mu\delta^3(\mathbf{r}-\mathbf{r_0})\mathbf{m}$. The electric and magnetic fields generated by this dipole in a homogeneous medium are given by expressions analogous to Eqs. (B1) and (B2) applied to the magnetic dipole case [51]:

$$\mathbf{H}^{\mathrm{MD}} = \nabla(\nabla\cdot\boldsymbol{\pi}_m) + k^2\boldsymbol{\pi}_m, \quad \mathbf{E}^{\mathrm{MD}} = i\omega\mu\nabla\times\boldsymbol{\pi}_m,$$

where this time $\boldsymbol{\pi}_m$ is the magnetic Hertz potential [51] and it can be calculated as

$$\boldsymbol{\pi}_m = \mathbf{m}\frac{e^{ik|\mathbf{r}-\mathbf{r_0}|}}{4\pi|\mathbf{r}-\mathbf{r_0}|}.$$

Proceeding in same manner as for the electric dipole, the magnetic field $\mathbf{H}^{\mathrm{MD}}$ and the electric field $\mathbf{E}^{\mathrm{MD}}$ can then be written as

$$\mathbf{H}^{\mathrm{MD}} = \frac{i}{8\pi^2}\iint\frac{1}{k_z}e^{i(k_x x+k_y y)}e^{ik_z|z-z_0|}\mathbf{f}_H dk_x dk_y,$$

$$\mathbf{E}^{\mathrm{MD}} = -\frac{i\omega\mu}{8\pi^2}\iint\frac{1}{k_z}e^{i(k_x x+k_y y)}e^{ik_z|z-z_0|}\mathbf{f}_E dk_x dk_y,$$

where

$$\mathbf{f}_H = k^2\mathbf{m} - \mathbf{k}^{\pm}(\mathbf{k}^{\pm}\cdot\mathbf{m}), \quad \mathbf{f}_E = \mathbf{k}^{\pm}\times\mathbf{m},$$

with the same definition for $\mathbf{k}^{\pm}$ as given before. In the same manner as for the electric dipole, we can then project the functions $\mathbf{f}_E$ and $\mathbf{f}_H$ along the two directions relative to the s and p polarizations so that they can be expressed as

$$\mathbf{f}_E = \nu_s^{\pm}\hat{\mathbf{e}}_s + \nu_p\hat{\mathbf{e}}_p^{\pm},$$

$$\mathbf{f}_H = k\nu_p\hat{\mathbf{e}}_s - k\nu_s^{\pm}\hat{\mathbf{e}}_p^{\pm},$$

where

$$\nu_s^{\pm} = \mathbf{f}_E\cdot\hat{\mathbf{e}}_s = \pm\frac{(k_x m_x + k_y m_y)k_z}{\sqrt{k_x^2+k_y^2}} - \sqrt{k_x^2+k_y^2}\,m_z,$$

$$\nu_p = \mathbf{f}_E\cdot\hat{\mathbf{e}}_p^{\pm} = \frac{k}{\sqrt{k_x^2+k_y^2}}(k_y m_x - k_x m_y).$$

The s-polarized fields of the magnetic dipole are then given by

$$\mathbf{H}_s^{\mathrm{MD}}(k_x,k_y)|_{z=z_0} = \frac{i}{8\pi^2}k\left[\pm\frac{1}{\sqrt{k_x^2+k_y^2}}(k_x m_x + k_y m_y) - \frac{1}{k_z}\sqrt{k_x^2+k_y^2}\,m_z\right]\hat{\mathbf{e}}_p^{\pm},$$

$$\mathbf{E}_s^{\mathrm{MD}}(k_x,k_y)|_{z=z_0} = -\frac{i\omega\mu}{8\pi^2}\left[\pm\frac{1}{\sqrt{k_x^2+k_y^2}}(k_x m_x + k_y m_y) - \frac{1}{k_z}\sqrt{k_x^2+k_y^2}\,m_z\right]\hat{\mathbf{e}}_s,$$

and the p-polarized fields are given by

$$\mathbf{H}_p^{\mathrm{MD}}(k_x,k_y)|_{z=z_0} = -\frac{i}{8\pi^2}k\left[\frac{k}{k_z\sqrt{k_x^2+k_y^2}} \times (-k_y m_x + k_x m_y)\right]\hat{\mathbf{e}}_s,$$

$$\mathbf{E}_p^{\mathrm{MD}}(k_x,k_y)|_{z=z_0} = \frac{i\omega\mu}{8\pi^2}\left[\frac{k}{k_z\sqrt{k_x^2+k_y^2}} \times (-k_y m_x + k_x m_y)\right]\hat{\mathbf{e}}_p^{\pm}.$$

Notice that these fields can be written as

$$\mathbf{E}^{\mathrm{MD}}(k_x,k_y)|_{z=z_0} = \frac{i}{8\pi^2\varepsilon}\frac{k^2}{k_z}\frac{1}{c}[-(\hat{\mathbf{e}}_p^{\pm}\cdot\mathbf{m})\hat{\mathbf{e}}_s + (\hat{\mathbf{e}}_s\cdot\mathbf{m})\hat{\mathbf{e}}_p^{\pm}],$$

$$\mathbf{H}^{\mathrm{MD}}(k_x,k_y)|_{z=z_0} = \frac{i\omega}{8\pi^2}\frac{k}{k_z}\frac{1}{c}[(\hat{\mathbf{e}}_p^{\pm}\cdot\mathbf{m})\hat{\mathbf{e}}_p^{\pm} + (\hat{\mathbf{e}}_s\cdot\mathbf{m})\hat{\mathbf{e}}_s].$$

As expected [51], going from the electric dipole to the magnetic one, we obtain the same result that we would obtain simply performing the following substitutions: $\varepsilon \to \mu$, $\mathbf{p} \to \mu\mathbf{m}$, $\mathbf{H} \to -\mathbf{E}$, $\mathbf{E} \to \mathbf{H}$.

APPENDIX D: REFLECTED FIELDS

The fields reflected from a surface can be easily calculated starting from the fields radiated by the dipole in a homogeneous medium. In fact, retrieving the reflected fields once the angular spectrum has been determined requires only knowledge of Fresnel's reflection coefficients $r_s(\omega,k_x,k_y)$ and $r_p(\omega,k_x,k_y)$, characteristic of the specific reflective material or layered media. The reflected electric and magnetic fields of both electric and magnetic dipoles can therefore be written as

$$\begin{aligned}
&\mathbf{E}_{\mathrm{ref}}^{\mathrm{ED}}(k_x,k_y,z) \\
&\quad= \frac{i}{8\pi^2\varepsilon}\frac{k^2}{k_z}[r_s(\hat{\mathbf{e}}_s\cdot\mathbf{p})\hat{\mathbf{e}}_s + r_p(\hat{\mathbf{e}}_p^{-}\cdot\mathbf{p})\hat{\mathbf{e}}_p^{+}]e^{ik_z(z+z_0)}, \\
&\mathbf{H}_{\mathrm{ref}}^{\mathrm{ED}}(k_x,k_y,z) \\
&\quad= \frac{i\omega}{8\pi^2}\frac{k}{k_z}[r_p(\hat{\mathbf{e}}_p^{-}\cdot\mathbf{p})\hat{\mathbf{e}}_s - r_s(\hat{\mathbf{e}}_s\cdot\mathbf{p})\hat{\mathbf{e}}_p^{+}]e^{ik_z(z+z_0)}, \\
&\mathbf{E}_{\mathrm{ref}}^{\mathrm{MD}}(k_x,k_y,z) \\
&\quad= \frac{i}{8\pi^2\varepsilon}\frac{k^2}{k_z}\frac{1}{c}[-r_s(\hat{\mathbf{e}}_p^{-}\cdot\mathbf{m})\hat{\mathbf{e}}_s + r_p(\hat{\mathbf{e}}_s\cdot\mathbf{m})\hat{\mathbf{e}}_p^{+}]e^{ik_z(z+z_0)}, \\
&\mathbf{H}_{\mathrm{ref}}^{\mathrm{MD}}(k_x,k_y,z) \\
&\quad= \frac{i\omega}{8\pi^2}\frac{k}{k_z}\frac{1}{c}[r_p(\hat{\mathbf{e}}_s\cdot\mathbf{m})\hat{\mathbf{e}}_s + r_s(\hat{\mathbf{e}}_p^{-}\cdot\mathbf{m})\hat{\mathbf{e}}_p^{+}]e^{ik_z(z+z_0)}.
\end{aligned} \tag{D1}$$

If the surface or layered media are rotationally symmetric around z, the reflection coefficients will have the same symmetry. They will depend only on k_t, independent of the angle, and therefore, the directionality of the fields reflected by the surface (which includes any excited guided modes) will not be affected by the surface. The directionality will be entirely determined by that of the dipole in the homogeneous medium.

It is worth noticing that these expressions are mathematically general and allow using any Fresnel reflection coefficients. In particular, no assumption is made on the value of frequency ω radiated by the dipole, so we can consider the response to complex frequencies for which the guided modes can show interesting effects such as the lack of back bending of surface plasmons [53,54]. These properties are fully described via Fresnel's coefficient of the surface using a complex ω.

[1] F. J. Rodríguez-Fortuño, G. Marino, P. Ginzburg, D. O'Connor, A. Martinez, G. A. Wurtz, and A. V. Zayats, Near-field interference for the unidirectional excitation of electromagnetic guided modes, Science **340**, 328 (2013).

[2] P. V. Kapitanova, P. Ginzburg, F. J. Rodríguez-Fortuño, D. S. Filonov, P. M. Voroshilov, P. A. Belov, A. N. Poddubny, Y. S. Kivshar, G. A. Wurtz, and A. V. Zayats, Photonic spin Hall effect in hyperbolic metamaterials for polarization-controlled routing of subwavelength modes, Nat. Commun. **5**, 3226 (2014).

[3] A. Aiello, P. Banzer, M. Neugebauer, and G. Leuchs, From transverse angular momentum to photonic wheels, Nat. Photonics **9**, 789 (2015).

[4] A. Espinosa-Soria and A. Martinez, Transverse spin and spin-orbit coupling in silicon waveguides, IEEE Photonics Technol. Lett. **28**, 1561 (2016).

[5] T. Van Mechelen and Z. Jacob, Universal spin-momentum locking of evanescent waves, Optica **3**, 118 (2016).

[6] R. J. Coles, D. M. Price, J. E. Dixon, B. Royall, E. Clarke, P. Kok, M. S. Skolnick, A. M. Fox, and M. N. Makhonin, Chirality of nanophotonic waveguide with embedded quantum emitter for unidirectional spin transfer, Nat. Commun. **7**, 11183 (2016).

[7] B. Le Feber, N. Rotenberg, and L. Kuipers, Nanophotonic control of circular dipole emission, Nat. Commun. **6**, 6695 (2015).

[8] I. J. Luxmoore, N. A. Wasley, A. J. Ramsay, A. C. T. Thijssen, R. Oulton, M. Hugues, S. Kasture, V. G. Achanta, A. M. Fox, and M. S. Skolnick, Interfacing Spins in an InGaAs Quantum Dot to a Semiconductor Waveguide Circuit Using Emitted Photons, Phys. Rev. Lett. **110**, 037402 (2013).

[9] L. Marrucci, Quantum optics: Spin gives direction, Nat. Phys. **11**, 9 (2014).

[10] R. J. Coles, N. Prtljaga, B. Royall, I. J. Luxmoore, A. M. Fox, and M. S. Skolnick, Waveguide-coupled photonic crystal cavity for quantum dot spin readout, Opt. Express **22**, 2376 (2014).

[11] R. Mitsch, C. Sayrin, B. Albrecht, P. Schneeweiss, and A. Rauschenbeutel, Quantum state-controlled directional spontaneous emission of photons into a nanophotonic waveguide, Nat. Commun. **5**, 5713 (2014).

[12] A. B. Young, A. C. T. Thijssen, D. M. Beggs, P. Androvitsaneas, L. Kuipers, J. G. Rarity, S. Hughes, and R. Oulton, Polarization Engineering in Photonic Crystal Waveguides for Spin-Photon Entanglers, Phys. Rev. Lett. **115**, 153901 (2015).

[13] P. Lodahl, S. Mahmoodian, S. Stobbe, P. Schneeweiss, J. Volz, A. Rauschenbeutel, H. Pichler, and P. Zoller, Chiral quantum optics, Nature (London) **541**, 473 (2017).

[14] J. Petersen, J. Volz, and A. Rauschenbeutel, Chiral nanophotonic waveguide interface based on spin-orbit interaction of light, Science **346**, 67 (2014).

[15] D. O'Connor, P. Ginzburg, F. J. Rodríguez-Fortuño, Ga. Wurtz, and A. V. Zayats, Spin-orbit coupling in surface plasmon scattering by nanostructures, Nat. Commun. **5**, 5327 (2014).

[16] M. Neugebauer, T. Bauer, P. Banzer, and G. Leuchs, Polarization tailored light driven directional optical nanobeacon, Nano Lett. **14**, 2546 (2014).

[17] M. Neugebauer, T. Bauer, A. Aiello, and P. Banzer, Measuring the Transverse Spin Density of Light, Phys. Rev. Lett. **114**, 063901 (2015).

[18] K. Y. Bliokh, F. J. Rodríguez-Fortuño, F. Nori, and A. V. Zayats, Spin-orbit interactions of light, Nat. Photonics **9**, 796 (2015).

[19] F. Cardano and L. Marrucci, Spin-orbit photonics, Nat. Photonics **9**, 776 (2015).

[20] L. Marrucci, E. Karimi, S. Slussarenko, B. Piccirillo, E. Santamato, E. Nagali, and F. Sciarrino, Spin-to-orbital conversion of the angular momentum of light and its classical and quantum applications, J. Opt. **13**, 064001 (2011).

[21] X. Yin, Z. Ye, J. Rho, Y. Wang, and X. Zhang, Photonic spin hall effect at metasurfaces, Science **339**, 1405 (2013).

[22] A. Espinosa-Soria, F. Rodríguez-Fortuño, A. Griol, and A. Martínez, On-chip optimal stokes nanopolarimetry based on spin-orbit interaction of light, Nano Lett. **17**, 3139 (2017).

[23] F. J. Rodríguez-Fortuño, D. Puerto, A. Griol, L. Bellieres, J. Martí, and A. Martínez, Universal method for the synthesis of arbitrary polarization states radiated by a nanoantenna, Laser Photonics Rev. **8**, L27 (2014).

[24] F. J. Rodríguez-Fortuño, I. Barber-Sanz, D. Puerto, A. Griol, and A. Martínez, Resolving light handedness with an on-chip silicon microdisk, ACS Photonics **1**, 762 (2014).

[25] F. J. Rodríguez-Fortuño, D. Puerto, A. Griol, L. Bellieres, J. Martí, and A. Martínez, Sorting linearly polarized photons with a single scatterer, Opt. Lett. **39**, 1394 (2014).

[26] S. B. Wang and C. T. Chan, Lateral optical force on chiral particles near a surface, Nat. Commun. **5**, 3307 (2014).

[27] A. Hayat, J. P. B. Mueller, and F. Capasso, Lateral chirality—Sorting optical forces, Proc. Natl. Acad. Sci. U.S.A. **112**, 13190 (2015).

[28] F. J. Rodríguez-Fortuño, N. Engheta, A. Martínez, and A. V. Zayats, Lateral forces on circularly polarizable particles near a surface, Nat. Commun. **6**, 8799 (2015).

[29] S. Sukhov, V. Kajorndejnukul, R. Rezvani Naraghi, and A. Dogariu, Dynamic consequences of optical spin-interaction, Nat. Photonics **9**, 809 (2015).

[30] S. Scheel, S. Y. Buhmann, C. Clausen, and P. Schneeweiss, Directional spontaneous emission and lateral Casimir-Polder force on an atom close to a nanofiber, Phys. Rev. A **92**, 043819 (2015).

[31] F. Kalhor, T. Thundat, and Z. Jacob, Universal spin-momentum locked optical forces, Appl. Phys. Lett. **108**, 061102 (2016).

[32] C. Sayrin, C. Junge, R. Mitsch, B. Albrecht, D. O'Shea, P. Schneeweiss, J. Volz, and A. Rauschenbeutel, Nanophotonic Optical Isolator Controlled by the Internal State of Cold Atoms, Phys. Rev. X **5**, 041036 (2015).

[33] A. I. Kuznetsov, A. E. Miroshnichenko, Y. Hsing Fu, J. Zhang, and B. Luk'yanchuk, Magnetic light, Sci. Rep. **2**, 492 (2012).

[34] U. Zywietz, A. B. Evlyukhin, C. Reinhardt, and B. N. Chichkov, Laser printing of silicon nanoparticles with resonant optical electric and magnetic responses, Nat. Commun. **5**, 3402 (2014).

[35] F. L. Kien, V. I. Balykin, and K. Hakuta, Angular momentum of light in an optical nanofiber, Phys. Rev. A **73**, 053823 (2006).

[36] F. L. Kien and A. Rauschenbeutel, Anisotropy in scattering of light from an atom into the guided modes of a nanofiber, Phys. Rev. A **90**, 023805 (2014).

[37] C. Junge, D. O'Shea, J. Volz, and A. Rauschenbeutel, Strong Coupling Between Single Atoms and Nontransversal Photons, Phys. Rev. Lett. **110**, 213604 (2013).

[38] K. Y. Bliokh, D. Smirnova, and F. Nori, Quantum spin Hall effect of light, Science **348**, 1448 (2015).

[39] J. D. Jackson, *Classical Electrodynamics* (Wiley, New York, 1999).

[40] S. E. Sund, J. A. Swanson, and D. Axelrod, Cell membrane orientation visualized by polarized total internal reflection fluorescence, Biophys. J. **77**, 2266 (1999).

[41] K. Y. Bliokh and F. Nori, Transverse spin of a surface polariton, Phys. Rev. A **85**, 061801 (2012).

[42] K. Y. Bliokh, A. Y. Bekshaev, and F. Nori, Extraordinary momentum and spin in evanescent waves, Nat. Commun. **5**, 3300 (2014).

[43] L. Novotny and B. Hecht, *Principles of Nano-optics* (Cambridge University Press, Cambridge, 2012).

[44] N. Rotenberg, M. Spasenović, T. L. Krijger, B. Le Feber, F. J. García de Abajo, and L. Kuipers, Plasmon Scattering from Single Subwavelength Holes, Phys. Rev. Lett. **108**, 127402 (2012).

[45] S. Scheel and S. Y. Buhmann, Macroscopic quantum electrodynamics-concepts and applications, Acta Phys. Slovaca **58**, 675 (2008).

[46] See Supplemental Material at http://link.aps.org/supplemental/10.1103/PhysRevB.95.245416 for the animated version of Fig. 5.

[47] B. García-Cámara, F. Moreno, F. González, and O. J. F. Martin, Light scattering by an array of electric and magnetic nanoparticles, Opt. Express **18**, 10001 (2010).

[48] S. Person, M. Jain, Z. Lapin, S. J. Jose, G. Wicks, and L. Novotny, Demonstration of zero optical backscattering from single nanoparticles, Nano Lett. **13**, 1806 (2013).

[49] I. Staude, A. E. Miroshnichenko, M. Decker, N. T. Fofang, S. Liu, E. Gonzales, J. Dominguez, T. S. Luk, D. N. Neshev, I. Brener *et al.*, Tailoring directional scattering through magnetic and electric resonances in subwavelength silicon nanodisks, ACS Nano **7**, 7824 (2013).

[50] A. B. Evlyukhin and S. I. Bozhevolnyi, Resonant unidirectional and elastic scattering of surface plasmon polaritons by high refractive index dielectric nanoparticles, Phys. Rev. B **92**, 245419 (2015).

[51] A. Ishimaru, *Electromagnetic Wave Propagation, Radiation, and Scattering* (Prentice Hall, Englewood Cliffs, NJ, 1991).

[52] L. Mandel and E. Wolf, *Optical Coherence and Quantum Optics* (Cambridge University Press, Cambridge, 1995).

[53] A. Archambault, M. Besbes, and J.-J. Greffet, Superlens in the Time Domain, Phys. Rev. Lett. **109**, 097405 (2012).

[54] K. L. Tsakmakidis, T. W. Pickering, J. M. Hamm, A. F. Page, and O. Hess, Completely Stopped and Dispersionless Light in Plasmonic Waveguides, Phys. Rev. Lett. **112**, 167401 (2014).